

# Fast evaluation of the current drive efficiency by electron cyclotron waves for reactor studies

Emanuele Poli<sup>1,\*</sup>, Maximilian Müller<sup>1</sup>, Hartmut Zohm<sup>1</sup>, and Michael Kovari<sup>2</sup>

<sup>1</sup>Max-Planck-Institut für Plasmaphysik, Garching bei München, Germany

<sup>2</sup>CCFE, Culham Science Centre, Abingdon, UK

**Abstract.** The determination of the current driven by electron cyclotron waves is usually performed employing ray/beam tracing codes, which require as an input the magnetic equilibrium, the electron density and the electron temperature profiles on one side and the beam injection parameters on the other. In the frame of systems-code applications, however, a different approach is needed, as some of the required input quantities are not available. Here, a procedure to evaluate the achievable ECCD efficiency for given global reactor parameters is proposed. It relies on a single numerical evaluation of the current drive efficiency (based on the adjoint method and including momentum-conserving corrections) for suitably chosen input values. The results are shown to be in good agreement with the full numerical optimization of the ECCD efficiency for a number of reactor-relevant scenarios. As described in this paper, this approach does not include the effect of parasitic absorption from higher cyclotron harmonics, which becomes important starting from electron temperatures of the order of 30 keV.

## 1 Introduction

The calculation of the current driven by auxiliary heating systems is just a small part of the operations performed by systems codes like PROCESS [1, 2] in order to assess the performance of a fusion reactor for a given set of global parameters. While in most applications electron-cyclotron current drive (ECCD) is calculated by ray/beam tracing codes [3] employing as an input some given values for the magnetic equilibrium (two-dimensional in tokamaks), the density and the electron temperature profiles (one-dimensional), and the EC beam parameters (launch position, angles and frequency), in a systems code some of these data are not available. In particular, the antenna parameters which would yield the optimum current drive for a given set of global parameters are not known. This makes the usual strategy based on tracing the beam path through the plasma and exploring the relevant parameter space [4] not applicable, even if the numerical burden were manageable. In this contribution, a procedure is proposed to evaluate the current driven by EC waves through a single numerical determination of the ECCD efficiency according to the adjoint method [5] for a suitably selected set of input values deduced from the global machine parameters. The related predictions are compared to extensive optimization loops performed with the code TORBEAM [6, 7] for a number of reactor-relevant scenarios. The computational effort of the proposed approach, which amounts basically to the numerical quadrature of two one-dimensional integrals (one integrand being itself

known in integral form), is assumed here to be affordable within systems code applications.

## 2 Theoretical background

In order to establish the notation and introduce the discussion to follow, the basic features of the interaction between EC waves and electrons around the cyclotron resonance (or one of its harmonics) are recalled in this section. The energy carried by the wave is transferred to the particles in the plasma satisfying the relativistic resonance condition [8])

$$\omega - \frac{n\Omega}{\gamma} - k_{\parallel}v_{\parallel} = 0, \quad (1)$$

where  $\omega$  is the frequency of the injected wave,  $n$  is the harmonic number,  $\Omega = eB/m$  is the cyclotron frequency of the electrons,  $\gamma = \sqrt{1 + u_{\parallel}^2 + u_{\perp}^2}$  is the relativistic Lorentz factor (with  $\mathbf{u} = \mathbf{p}/mc$  the normalized momentum) and  $k_{\parallel}$  is the component of the wave vector parallel to the magnetic field. Introducing  $N_{\parallel} = ck_{\parallel}/\omega$  and  $\bar{\Omega} = \Omega/\omega$ , the resonance condition becomes

$$\gamma - N_{\parallel}u_{\parallel} - n\bar{\Omega} = 0. \quad (2)$$

In momentum space, the resonance curve for given values of  $\bar{\Omega}$  and  $N_{\parallel}$  is hence a half-ellipse (only values  $u_{\perp} > 0$  are considered)

$$(1 - N_{\parallel}^2) \left( u_{\parallel} - \frac{N_{\parallel}}{1 - N_{\parallel}^2} n\bar{\Omega} \right)^2 + u_{\perp}^2 = \frac{n^2 \bar{\Omega}^2}{1 - N_{\parallel}^2} - 1. \quad (3)$$

\*e-mail: Emanuele.Poli@ipp.mpg.de

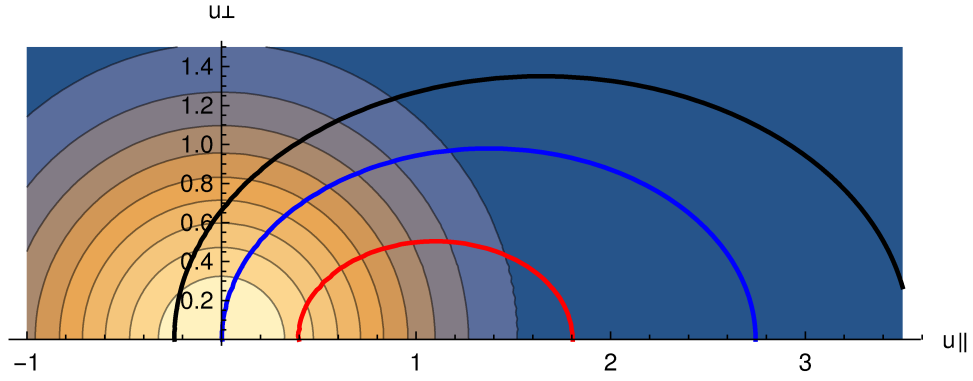


**Figure 1.** Relativistic resonance curves for  $N_{\parallel} = 0.7$  and different values of  $\bar{\Omega}$  (red:  $\bar{\Omega} = 0.8$ ; blue:  $\bar{\Omega} = 1$ ; black:  $\bar{\Omega} = 1.2$ ). Maxwellian isocontours centred at  $(u_{\parallel}, u_{\perp}) = (0, 0)$  are also shown.

which intersects the  $u_{\parallel}$ -axis at

$$u_{\parallel\mp} = \frac{nN_{\parallel}\bar{\Omega} \mp \sqrt{n^2\bar{\Omega}^2 - (1 - N_{\parallel}^2)}}{1 - N_{\parallel}^2}. \quad (4)$$

The resonance condition for a given harmonic  $n$  can be satisfied if

$$n\bar{\Omega} = \sqrt{1 - N_{\parallel}^2} \quad (5)$$

or for larger values of  $n\bar{\Omega}$ . For low-field side (LFS) injection, Eq.(5) defines the so-called pinch point [9] as the first point in resonance

$$u_{\parallel pp} = \frac{nN_{\parallel}\bar{\Omega}}{1 - N_{\parallel}^2} = \frac{N_{\parallel}}{\sqrt{1 - N_{\parallel}^2}} \quad (6)$$

which can be seen as a degenerate case of the ellipse given by Eq.(3).

Fig. 1 shows the resonance ellipses for three different values of  $\bar{\Omega}$ . Also shown are the contour levels of a Maxwell distribution function centred at the origin. The strongest wave-particle interaction can be assumed to take place around  $u_{\parallel-}$ , the lower intercept of the resonance curve with the  $u_{\parallel}$ -axis, as this is the point on the resonance curve where most electrons are available (for scenarios with negative  $N_{\parallel}$ , the role of  $u_{\parallel-}$  and  $u_{\parallel+}$  is swapped and the strongest interaction is localized around  $u_{\parallel+}$ ). For a given harmonic, the position of  $u_{\parallel-}$  decreases (for LFS injection schemes) from the pinch point to  $u_{\parallel} = 0$  (if the cold resonance  $\bar{\Omega} = 1$  is reached) and then crosses the origin. Since the collisionality decreases with increasing particle energy  $\mathcal{E} = mc^2(\gamma - 1)$ , optimum ECCD conditions are reached when sufficient absorption is provided on high-velocity electrons, as discussed in the following.

### 3 ECCD Optimization

Since the energy range of the resonant electrons is crucial for this study, here the electron energy for a standard ECCD application (injection onto the  $q = 3/2$ -surface with frequency 170 GHz as foreseen in ITER for

neoclassical-tearing-mode stabilization [10]) is compared with that of a maximum-ECCD case, see Fig. 2. In the latter case, the optimum ECCD conditions have been found by scanning the injection angles for different positions of the antenna and different wave frequencies [4]. For the stabilization of neoclassical tearing modes, where a good localization of the deposited power is beneficial [11], the wave energy is deposited on slower electrons ( $\mathcal{E}/T_e \lesssim 2$ ), the absorption is strong and the radial extent of the absorption region is small (left panel). On the contrary, under conditions of high current drive, the wave-particle resonance is satisfied on electrons whose energy is several times larger than the electron temperature (right panel). As the number of electrons with such a high energy is low, the absorption is distributed across a much wider radial range. It is noticed that the optimum-ECCD case requires a wave frequency of 210 GHz, confirming previous studies [9]. The reason for this high frequency can be understood by recalling Eq.(6), which shows that increasing  $N_{\parallel}$  shifts the resonance to higher  $u_{\parallel}$  and hence increases the energy of the current-carrying electrons. Since parallel refractive index and wave frequency are connected at the pinch point through Eq.(5), a high value of  $N_{\parallel}$  must be accompanied by an increase in the wave frequency in order to ensure that the resonance does not move into the LFS.

It is interesting to note that the energy of the resonant electrons at the position of maximum absorption, defined as the position along the beam axis at which the transfer of energy from the wave to the plasma is highest and marked by a black cross in Fig 2, is found for a value of  $\mathcal{E}/T_e \equiv f_T \approx 4$  under conditions of optimum ECCD (here  $\mathcal{E}$  is defined as  $mc^2(\sqrt{1 + u_{\parallel-}^2} - 1)$ , according to the discussion in the previous section, and  $T_e$  is the electron temperature), as shown by the black cross in the right panel of Fig. 2. An analysis of other reactor-relevant plasma scenarios (see parameters in Table 1) leads to similar values of  $\mathcal{E}/T_e$  for resonant electrons around the location of maximum absorption. This can be explained by the fact that optimum current drive is achieved by moving the resonance to the highest electron energies still compatible with sufficient absorption, as discussed above. As shown in [12],

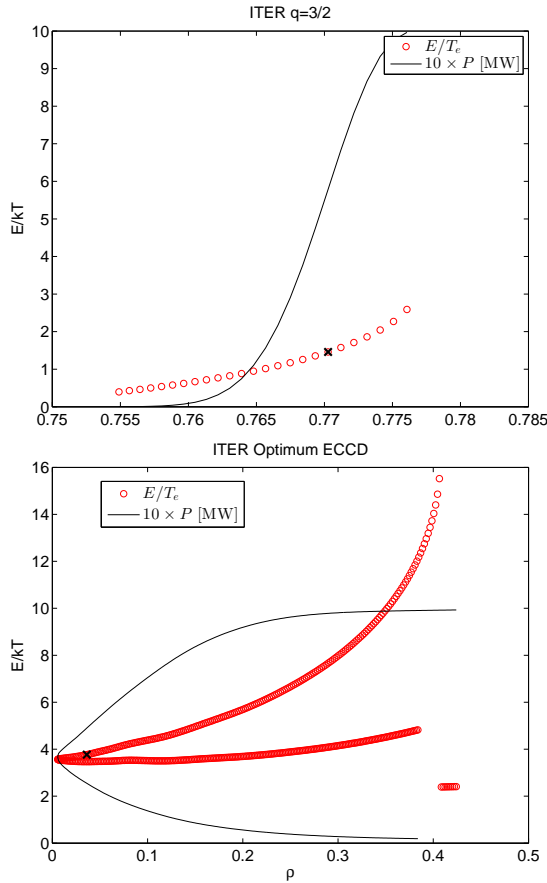


**Figure 2.** Comparison of the energy of the resonant electrons (calculated as  $\mathcal{E} = mc^2(\gamma - 1)$  with  $\gamma = \sqrt{1 + u_{||-}^2}$ , see text), normalized to the electron temperature, for a standard ITER situation (deposition on the  $q = 3/2$ -surface, injected frequency 170 GHz, launch position  $(R, Z) = (705.4, 417.8)$  cm, toroidal injection angle  $\beta = 20^\circ$ , left panel) and an ITER high-CD scenario (central deposition, injected frequency 210 GHz, launch position  $(R, Z) = (810, 320)$  cm, toroidal injection angle  $\beta = 37^\circ$ , right panel). The black crosses denote the position of maximum absorption. Also shown is the power carried by the beam, multiplied by 10 for the ease of comparison (black curves).

estimating analytically the absorption coefficient for the O-mode at the fundamental harmonic and imposing that the absorption takes place within a given fraction  $\Delta\rho$  of the minor radius of the machine one can determine the maximum energy of the resonant electrons as a function of the plasma parameters. Imposing  $\Delta\rho \simeq 0.2$  leads to a ratio  $\mathcal{E}/T_e \simeq 4$  for values of temperature, density and magnetic field typically envisaged for a reactor. This condition is used in the approach described in the next section to fix the electron energy in the resonance condition and thus impose a constraint on  $\omega$  and  $N_{||}$ .

#### 4 Evaluation of the optimum ECCD efficiency from global parameters

As explained in Sec. 1, an extensive search for the maximum achievable ECCD efficiency is not feasible within the optimization loop typical of reactor systems

codes, because of the related numerical burden and because these codes do not provide, as a rule, the input needed by ray/beam tracing codes. The procedure adopted here with the aim of evaluating the efficiency achievable by ECCD for given global plasma parameters relies on a single numerical evaluation of the current drive efficiency, as implemented in the routine written by Lin-Liu for the TORAY-GA code [13], modified to include the momentum-conserving scheme developed by Marushchenko [14]. The parameters for the call are determined around the point of maximum absorption, since the procedure described at the end of the previous section provides a constraint on the energy of the resonant electrons at that position. Now we discuss how to determine the values of  $\omega$  and  $N_{||}$ . As it turns out, most of the input quantities needed by the current-drive routine can be inferred on the basis of the global parameters available from systems codes or calculated from the dispersion relation once  $\omega$  and  $N_{||}$  have been fixed.

Recalling the discussion in Sec. 2, it is assumed that the wave-particle interaction occurs around the low-energy end of the resonance curve, i.e. around  $u_{||-}$ . This allows also the determination of the relativistic factor in the resonance condition as  $\gamma = \sqrt{1 + u_{||-}^2}$ . From Eq.(2), the parallel refractive index can then be expressed as a function of the wave frequency as

$$N_{||} = \frac{1}{u_{||-}} \left( \sqrt{1 + u_{||-}^2} - \frac{n\Omega}{\omega} \right). \quad (7)$$

In order to determine  $\omega$ , one can invoke the requirement on the localization of the absorption employed to fix the electron energy. If  $R_a$  is the major-radius coordinate of the position of maximum absorption, the extension along  $R$  of the absorption region can be determined as  $\Delta R = a\Delta\rho \cos\chi$ , where  $a$  is the minor radius and  $\chi$  is the poloidal angle (measured from the midplane) of the absorption position. Since propagation from an elevated position is beneficial for ECCD in a reactor [4], the value of  $\chi$  has been fixed here to  $\chi = 60^\circ$ . Approximating now  $\Delta R$  with the distance  $R_{pp} - R_a$ , where  $R_{pp}$  is the major radius of the pinch point, one can determine the ratio  $R_{pp}/R_a$  as

$$\frac{R_{pp}}{R_a} = 1 + \frac{a\Delta\rho}{R_a} \cos\chi. \quad (8)$$

Assuming a scaling  $B \propto 1/R$ , the position  $R_{pp}$  fulfils by definition the relation

$$\frac{R_{pp}}{R_a} = \frac{n\Omega(R_a)}{\omega \sqrt{1 - N_{||}^2}}, \quad (9)$$

see Eq.(5). Assuming the absorption to be sufficiently localized that  $N_{||}$  can be taken as constant in the region of interest (as supported by beam tracing simulations), one can substitute Eq. (7), with  $\Omega = \Omega(R_a)$ , into the previous equation, to obtain a quadratic equation for the frequency shift  $\omega/n\Omega(R_a)$ . The relevant solution is

$$\frac{\omega}{n\Omega(R_a)} = \sqrt{1 + u_{||-}^2} + |u_{||-}| \sqrt{1 - \frac{R_a}{R_{pp}}}. \quad (10)$$

**Table 1.** Global tokamak parameters employed in the analysis of the ECCD efficiency. Additionally, a half-temperature DEMO1 case has been considered.

	DEMO1	DEMO2 nflat	DEMO2 npeak	ITER
$R_0$ [cm]	907	749.9	749.9	620
$a$ [cm]	292	288.5	288.5	201
$B_0$ [T]	5.66	5.627	5.627	5.3
$n_{e0}$ [ $10^{19} \text{ m}^{-3}$ ]	10.50	9.94	17.99	10.56
$T_{e0}$ [keV]	33.25	31.17	23.50	24.49
$Z_{\text{eff}}$	2	4.1823	4.13	1.7617

This determines in turn the value of  $N_{\parallel}$  through Eq. (7). Since  $\gamma = f_T T_e / mc^2 + 1$ , from the previous equations it results that the frequency shift increases nearly linearly with  $T_e$ , while  $N_{\parallel}$  scales with the square root of  $T_e$ . This result would suggest that higher and higher electron temperatures could be exploited to push the energy of the resonant electrons to higher and higher values (by correspondingly increasing  $N_{\parallel}$  and hence  $u_{\parallel pp}$ ) and thus improve the ECCD efficiency further and further. Unfortunately, the Doppler shift cannot be increased indefinitely because of the competing absorption of the next harmonic (for the scenarios considered here, the second O-mode harmonic), which limits the ECCD improvement with  $T_e$  to a range where the (local) temperature remains approximately below 30 keV [12]. This effect is still not included in the model described above.

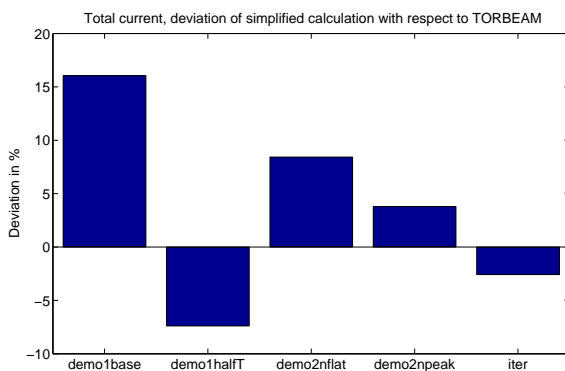


**Figure 3.** Deviation (in percent) between the estimated value of the current drive (calculated from a single evaluation of the ECCD efficiency, using Eqs. (7) and (10) to determine the required input) with respect to the current found in explicit beam tracing ECCD optimizations for the scenarios described in Table 1. The label demo1base (baseline) refers to the DEMO1 parameters reported in the table, while demo1halfT refers to the same case with the temperature divided by two.

Eqs. (7) and (10) have been implemented in a module which computes the input parameters needed for the numerical evaluation of the current drive efficiency. The

results are summarized in Fig. 3. For each of the scenarios considered here, it can be seen that the procedure described above matches closely the results of a complete TORBEAM optimization, the difference between the computed and the estimated current being below 15%. The highest deviation is found for the case with the highest temperature, as expected, and is originated by the lack of a model for the saturation of the ECCD efficiency at high temperatures, as discussed above. This limitation has been removed in a work performed after the preparation of the present paper [15]. It should be stressed that given the reduction of the computational burden (a single evaluation of the current drive efficiency as compared to an optimization over a multi-dimensional parameter space via complete beam-tracing calculations), an error of the order of 10% can be considered as satisfactory. Other parameters, in particular the wave frequency corresponding to maximum ECCD, are found to be estimated quite accurately by the present model as well.

## References

- [1] M. Kovari *et al.*, *Fus. Eng. Des.* **89**, 3054 (2014).
- [2] M. Kovari *et al.*, *Fus. Eng. Des.* **104**, 9 (2016).
- [3] R. Prater *et al.*, *Nucl. Fusion* **48**, 2349 (2008).
- [4] E. Poli *et al.*, *Nucl. Fusion* **53**, 013011 (2013).
- [5] T. M. Antonsen, K. R. Chu, *Phys. Fluids* **25**, 1295 (1982).
- [6] E. Poli *et al.*, *Comp. Phys. Comm.* **136**, 90 (2001).
- [7] E. Poli *et al.*, *Comp. Phys. Comm.* **225**, 36 (2018).
- [8] M. Bornatici *et al.*, *Nucl. Fusion* **23**, 1153 (1983).
- [9] R. W. Harvey *et al.*, *Nucl. Fusion* **37**, 69 (1997).
- [10] G. Ramponi *et al.*, *Nucl. Fusion* **48**, 054012 (2008).
- [11] H. Zohm *et al.*, *Plasma Phys. Control. Fusion* **49**, B341 (2007).
- [12] G. R. Smith *et al.*, *Phys. Fluids* **30**, 3633 (1987).
- [13] Y. R. Lin-Liu *et al.*, *Phys. Plasmas* **10**, 4064 (2003).
- [14] N. B. Marushchenko *et al.*, *Nucl. Fusion* **48**, 054002 (2008).
- [15] E. Poli *et al.*, *Phys. Plasmas* **25**, 122501 (2018).